Review

Emerging applicability of two-dimensional boron for energy catalysis

Dake ZHANG[1], Chengcheng ZHANG[1], Shenghua WANG[1], Wei SUN[1]✉

[1] *State Key Laboratory of Silicon Materials and Advanced Semiconductor Materials, School of Materials Science and Engineering, Zhejiang University, Hangzhou 310027, China*

Abstract: Due to their unique physical and chemical properties, two-dimensional (2D) boron nanosheets have received tremendous research attention and demonstrated substantial value in electronic devices, biomedicine, and energy conversion. In the preparation of boron nanosheets, compared with the bottom-up synthesis predominantly employed for electronics, the top-down synthesis route offers more facile and scalable production. In this mini-review, we mainly discuss the recent advances in the synthesis of boron nanosheets using the top-down strategy and the relevant applications in energy catalysis. Finally, inspired by our recent works on the novel applications of 2D silicon, we put forward prospects for designing boron nanosheets, providing insights into developing viable techniques for high-performance heterogeneous catalysis.

Keywords: 2D boron nanosheets; Top-down method; Catalytic applications

1 Introduction

Two-dimensional (2D) nanomaterials have received significant research interest in recent years owing to their unique physical and chemical attributes different from their bulk structure, such as large surface area, high carrier mobility, and excellent mechanical properties (Fan et al., 2021). During the past decade, various 2D nanomaterials were successfully synthesized, including silicene, MXenes, black phosphorus, graphene, and transition metal dichalcogenides (TMDs) (Han et al., 2022). These 2D nanomaterials found important application in sensors, biomedicine, electronics, and energy conversion and storage (Hou et al., 2023). Therefore, the continuous development of novel two-dimensional materials is a fascinating prospect for researchers.

Boron (B) is a neighbor of carbon in the periodic table, thus the two share many features. Thus, the question arises whether boron-based materials can be fabricated into 2D nanomaterials. In 2013, using first-principles calculations, Yakobson *et al.* predicted that B sheets can be synthesized on Ag (1 1 1) or Au (1 1 1) surfaces by deposition (Liu et al., 2013). In 2015, for the first time, Guisinger *et al.* employed the molecular beam epitaxy (MBE) method to experimentally grow boron sheets on silver surfaces under ultra-high vacuum conditions (Mannix et al., 2015). Subsequently, 2D boron was successfully synthesized on different metal substrates (including Cu, Au and Al) (Hou et al., 2020). Although these bottom-up methods for the synthesis of 2D boron have achieved great progress, the harsh preparation conditions and the limited production yield have impeded their large-scale application. By contrast, top-down strategies, including chemical exfoliation, cation exchange and physical exfoliation, have been found promising for preparing 2D boron in high quality and yield (Ji et al., 2018; Ou et al., 2021; Sun et al., 2023).

In this mini-review, we firstly discuss the top-down strategies for preparing 2D boron and its applications in energy catalysis from recent years. Then, the challenges and perspectives for future developments on 2D boron materials are outlined. Different from previous reviews focusing on bottom-up

✉ Wei SUN, sunnyway423@zju.edu.cn

🔟 Wei SUN, https://orcid.org/0000-0002-8525-619X

methods for 2D boron devices, this mini-review aims to provide useful insights into synthesizing scalable 2D boron and promotes new fields of application.

2 Synthesis of 2D boron using top-down strategies

2.1 Chemical exfoliation

Compared with epitaxial growth methods, the chemical exfoliation strategy is more extensive in preparing 2D nanomaterials owing to its simplicity, low cost, and high-yield characteristics. To date, most reported 2D nanomaterials obtained via chemical exfoliation have originated from materials with layered structures. Etching solvents (such as HCl, HF, and so on) can be used to break the interlayer bonding between the adjacent layers and thus obtain layered structures. For example, our group has successfully prepared various 2D silicon nanosheets by the chemical exfoliation method (Qian et al., 2018; Wang et al., 2022a). Furthermore, $CaSi_2$ was employed as a precursor and then the Ca^{2+} was deintercalated by concentrated hydrochloric or $CuCl_2$ (Wang et al., 2022b; Su et al., 2023).

MgB_2 is another layered ionic solid in which magnesium layers are sandwiched between two boron layers. The superconducting properties of this compound were reported in 2001, triggering huge research interest (Nagamatsu et al., 2001). The layered structure makes MgB_2 an excellent precursor for 2D boron synthesis. To extract the inter-layer magnesium (Mg) cations, as shown in Fig 1(a), Jasuja *et al*. employed ethylene diamine tetraacetic acid (EDTA) as a chelating agent to exfoliate the Mg atoms from bulk MgB_2 under magnetic stirring for an hour (James and Jasuja, 2017). The ICP-AES of boron-based nanosheets indicated a stoichiometric ratio (Mg: B) of 0.48:2, confirming the selective extraction of 52% Mg atoms. As shown in Fig. 1(b), atomic force microscopy (AFM) images revealed the 1.0-1.7 nm thickness of the obtained nanosheets. It is noteworthy that various functional groups (such as hydride, hy-

droxy and oxy-functional) were easily decorated on the surface of boron sheets due to the loss of Mg atoms (Fig. 1(c)). Jasuja *et al*. subsequently synthesized lamellas resembling "nanoaccordions" with a thickness in the range of 300-400 nm using sulfuric acid (H_2SO_4) and tetramethylammonium hydroxide (TMAOH) as exfoliation solvents in an ice bath for 72 h (Das and Jasuja, 2018). The purpose of applying TMAOH was to facilitate the expansion of layered crystals and then promote the delamination of MgB_2. Under ultrasonication in water, these nanoaccordions could be further transformed into few-layer thick (3-5 nm) 2D boron-based nanosheets. The obtained nanosheets were examined by ICP-AES and exhibited a stoichiometry of $Mg_{0.6}B_2$, suggesting that 40% of Mg atoms were excluded. To further extract Mg atoms from MgB_2, Liu *et al*. added I_2 into a mixture system composed of CH_3CN, HCl, and MgB_2, and stirred the mixture for 14 days under nitrogen gas protection to prepare few-layer Mg-deficient borophene nanosheets (FBN) (Zhang et al., 2022). HCl played an important role in etching Mg atom layers, and the negative charge of boron layers was reduced by oxidation with I_2, so that Mg layers could be deintercalated to the maximum extent (78%). Furthermore, based on the density functional theory, the authors proposed that the structure of 2D boron could not be maintained when the Mg atoms in the bulk MgB_2 were completely extracted, owing to the electron deficiency of boron atoms. Our research group employed concentrated HCl to etch MgB_2 under protective nitrogen gas atmosphere at room temperature for 24 h (Zhang et al., 2024). The obtained boron-based nanosheets exhibited a stoichiometry of $Mg_{0.12}B_2$, which is by far the highest deintercalation rate of Mg atoms compared to other reported boron-based nanosheets. This result may be attributed to the high concentration of HCl for extracting Mg atoms. Transmission Electron Microscopy (TEM) imaging showed that the thickness of the nanosheets was about 5 nm (Fig. 1(d)).
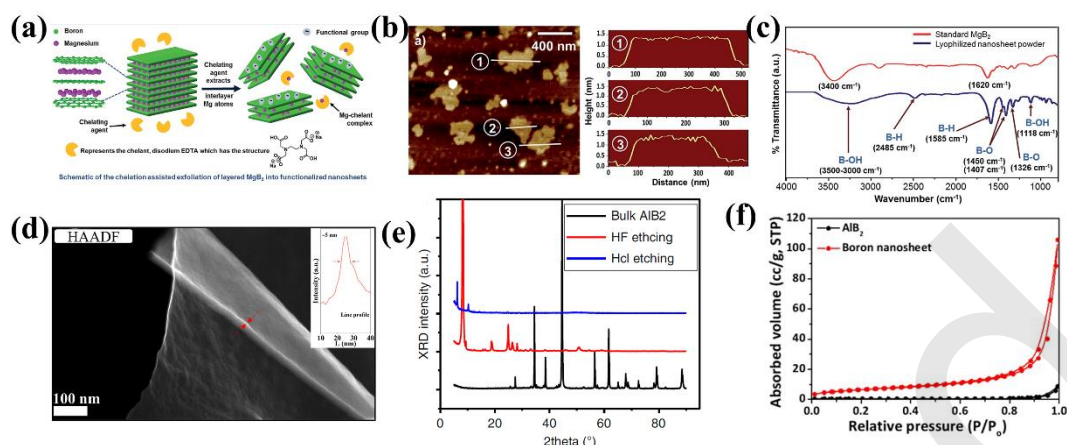
Fig. 1 (a) Schematic depicting the process of EDTA chelating a substantial fraction of interlayer Mg atoms. (b) AFM images of the obtained boron nanosheets. (c) Fourier-transform infrared spectroscopy (FT-IR) spectra of standard MgB_2 and boron nanosheets. (a-c) Reprinted from (James and Jasuja, 2017) (Copyright 2017, with permission from the Royal Society of Chemistry). (d) TEM image of the boron nanosheets. The inset image is the line profile at position "L". Reprinted from (Zhang, et al., 2024) (Copyright 2024, with permission from the Royal Society of Chemistry). (e) XRD patterns of bulk AlB_2, the boron product after HCl etching, and the aluminum product after HF etching. Reprinted from (Xie et al., 2022) (Copyright 2022, with permission from Springer Nature). (f) Nitrogen absorption-desorption isotherms of boron nanosheets and their precursor AlB_2. Reprinted from (Cai et al., 2022) (Copyright 2022, with permission from the Royal Society of Chemistry).

AlB_2 has a similar layered structure to MgB_2, indicating its potential value as a precursor for 2D boron synthesis. Zhang *et al.* employed different acids to selectively etch the AlB_2 precursor (Xie, et al., 2022). After HCl etching, the 2D boron nanosheets with 4 nm thickness were obtained. As shown in Fig. 1e, the main peak at $6°$ is the boron product in the X-ray diffraction (XRD) pattern, suggesting that Al atoms were exfoliated. By contrast, the main XRD peaks are AlF_3 and Al_2O_3 after HF etching, indicating that this step could completely remove the B element, leaving Al, O, and F behind. These results indicate that HCl is a suitable etching agent to exfoliate the AlB_2 precursor. Except for acid etching, an alkali solution is also a suitable etching agent to exfoliate bulk AlB_2 due to the strong binding ability between hydroxide radicals and the element Al. Li *et al.* employed a concentrated NaOH solution to etch AlB_2 under stirring at $70℃$ in a water bath for 12 h (Cai, et al., 2022). The obtained boron nanosheets with a thickness of 4 nm had a higher surface area (140.4 m^2/g) than pristine AlB_2 particles (4.1 m^2/g) (Fig. 1(f)).

2.2 Cation exchange with resin

2D boron nanosheets are easily furnished with many functional groups in the liquid phase exfoliation process. These can improve the stability of boron

nanosheets and tune their properties at the same time. Among them, hydrogen atom is a common element that attaches to the surface of boron sheets. After hydrogenation, the bonding of boron nanosheets can be restructured, so that the formed hydrogen boride (HB) will be stable in air or water.

In 2017, Kondo *et al.* prepared HB sheets (Fig. 2(a)) by the cation exchange method in methanol (or acetonitrile) at 343 K under an inert atmosphere for 3 days (Nishino et al., 2017a). Using an ion-exchange resin, the Mg atoms of MgB_2 were completely exchanged by protons, and the average yield of HB sheets as a yellow powder was 43.2%. The obtained HB sheets were estimated to have a thickness of approximately 0.5 nm. According to the results of thermal desorption spectroscopy (TDS), the B:H ratio in HB sheets was determined as 1:1 (Fig. 2(b)). It is noteworthy that the presence of $B(OH)_3$ as a byproduct could be detected during the synthetic process. To obtain unoxidized layered HB sheets, Kondo *et al.* developed an improved Schlenk method and obtained a pure HB sheet by ion-exchange reaction (Tominaka et al., 2020). Most importantly, the improved Schlenk method could effectively increase the yield of HB sheets from 43.2% to 60.2%, as shown in Fig. 2(c), a significant step toward for the mass production of boron nanosheets. Furthermore, to reduce the synthesis time of HB sheets while maintaining a high yield, Kondo *et al.* added formic

acid to the acetonitrile solution including MgB_2 powder and cation-exchange resin (Kawamura et al., 2020). As shown in Fig. 2(d), the formic acid acts as a mediator to facilitate ion exchange between protons in the ion-exchange resin and Mg atoms in MgB_2. Thus, this method took only 2 h of reaction time to achieve 50% yield, significantly faster than the conventional process taking 3 days.
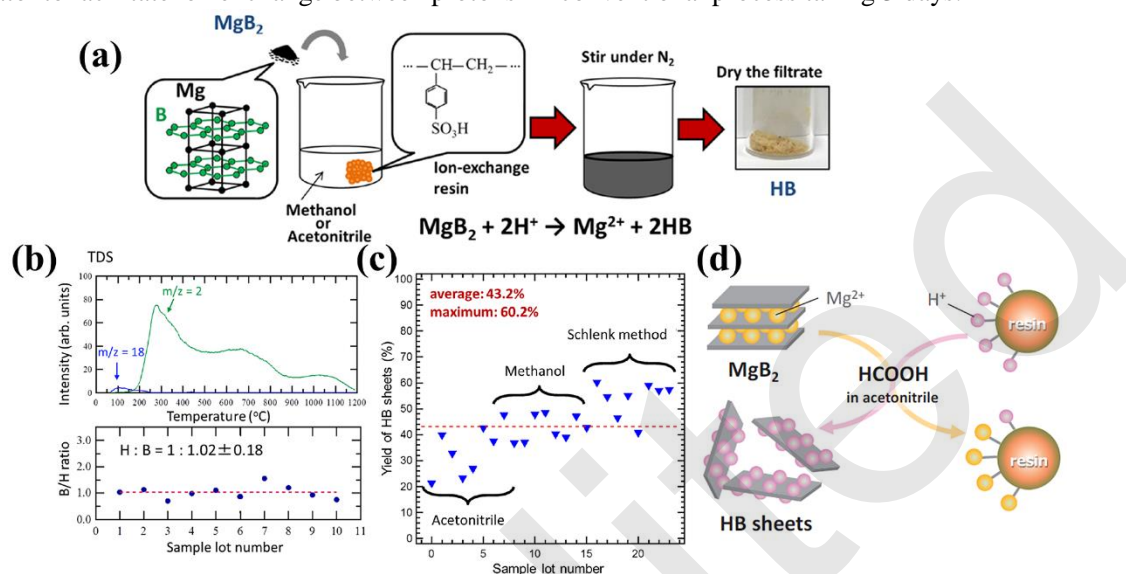

Fig. 2 (a) Schematic illustration of HB nanosheet preparation by a cation exchange process. (b) TDS of HB nanosheets. (a-b) Reprinted from (Nishino, et al., 2017a) (Copyright 2017, with permission from the American Chemical Society). (c) Yields of HB nanosheets using the conventional ion-exchange method with acetonitrile and methanol, and the Schlenk method with methanol. Reprinted from (Tominaka, et al., 2020) (Copyright 2020, with permission from Elsevier). (d) Schematic illustration of the synthesis of HB nanosheets facilitated by formic acid. Reprinted from (Kawamura, et al., 2020) (Copyright 2020, with permission from The Chemical Society of Japan).

2.3 Physical exfoliation

A convenient strategy to obtain 2D materials from bulk materials is the mechanical exfoliation method, which utilizes shear forces to overcome the weak van der Waals interactions between the connecting layers. In 2004, Geim *et al.* successfully synthesized monolayer and few-layer graphene from graphite by employing this method for the first time (Novoselov et al., 2004). Subsequently, various 2D materials were prepared by this approach, such as MoS_2, BP and WS_2 (Radisavljevic et al., 2011; Zhao et al., 2012; Liu et al., 2014). However, it was not until 2021 that Chahal *et al*. adopted it for the synthesis of 2D boron owing to the misunderstanding of the crystal structure of boron. The authors proposed that the failure of using scotch tape was due to the higher exfoliation energy of boron crystal than other bulk crystals (including MoS_2, Gr, and BP) calculated by DFT Fig. 3(a) (Chahal et al., 2021). Therefore, they employed double-sided foam tape as an alternative to exfoliate the boron crystal (Fig. 3(b)). Field-emission scanning electron microscopy (FESEM) indicated that the lateral dimensions of the obtained boron sheets were a few micrometers, but the straightened stiff sheets also seemed relatively thick (Fig. 3(c)).
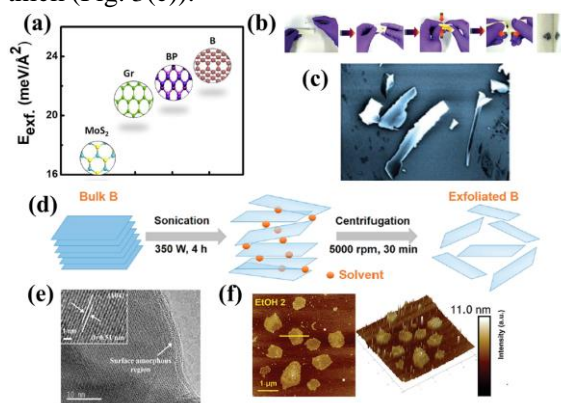

Fig. 3(a) Exfoliation energy of different materials (including MoS_2, Gr, BP, and B). (b) Digital images of the steps of the mechanical exfoliation of boron nanosheets using double-sided foam tape. (c) FESEM image of the obtained boron sheets. (a-c) Reprinted from (Chahal, et al., 2021) (Copyright 2021, with permission from Wiley). (d) Schematic illustration of the ultrasonication liquid exfoliation process. Reprinted from (Li et al., 2018) (Copyright 2018, with permission from the American Chemical Society). (e)

HRTEM image of the exfoliated boron nanosheets. Reprinted from (Ma et al., 2020) (Copyright 2020, with permission from the Royal Society of Chemistry). (f) AFM image of the exfoliated boron nanosheets in ethanol solvent. Reprinted from (Chand et al., 2022) (Copyright 2022, with permission from Wiley).

Despite the simplicity and cost-efficiency of mechanical exfoliation to prepare 2D materials, it has some shortcomings, such as large thickness and low yield, which fails to meet the demands of many technological applications. By contrast, the ultrasonication liquid exfoliation method has been recognized as an appealing route to produce 2D materials, due to its advantage that the size, quality, and yield of 2D materials can be controlled by the sonication solvent and time. In 2018, Teo and co-authors prepared few-layer boron sheets from bulk boron by the ultrasonication liquid method, as shown in Fig. 3(d) (Li, et al., 2018). They found that the obtained boron sheets had an average thickness of 1.8 nm by using dimethylformamide (DMF) as the exfoliation solvent. When isopropyl alcohol (IPA) was used instead, the thickness of boron sheets was 4.7 nm. Most importantly, the obtained boron nanosheets exhibited excellent stability in the exfoliating solvent over 50 days under ambient conditions, suggesting the enormous potential of this strategy for practical applications. Subsequently, Zhang *et al*. combined probe sonication and water bath sonication to prepare boron sheets from bulk boron precursor in IPA solvent (Ma, et al., 2020). As shown in Fig. 3(e), the HRTEM image confirmed the high crystalline nature of the exfoliated boron nanosheets. In addition, these sheets maintained good structural integrity and had a thickness of 2.1 nm and a lateral size of 82 nm. Meanwhile, in the above-mentioned works, ultrafine pure boron powder was used as the precursor, increasing the cost. Recently, Krishnan and co-workers prepared ultrathin boron nanosheets from low-cost bulk boron chunks by combining mechanical grinding and ultrasonication liquid exfoliation methods (Chand, et al., 2022). The yield of boron sheets from the ethanol solvent was 15 mg per 300 mg bulk boron, showcasing its efficiency and low cost to synthesize boron sheets. The AFM results showed that the obtained born nanosheets had a thickness of 5.5 nm in ethanol solvent (Fig. 3(f)).

In addition to bulk boron as the precursor, the layered compound of MgB_2 can also be exfoliated into boron-based sheets by the ultrasonication liquid method. In 2015, Das *et al*. found that 2D boron-based nanosheets could be synthesized from MgB_2 in the presence of water by ultrasonication for 30 min (Das et al., 2015). The obtained nanosheets exhibited a magnesium-deficient stoichiometry and were functionalized with hydroxyl groups, thus they were not pure boron nanosheets. To explore the reaction mechanism between MgB_2 and water, Kondo *et al*. revealed that there are mainly two steps in this reaction (Nishino et al., 2017b). First, there is an ion-exchange between protons and Mg cations. Second, the Mg-deficient boron hydride sheets and water undergo a hydrolysis reaction to produce H_2 and Mg-deficient hydroxyl-functionalized boron nanosheets.

3 Catalytic functions of 2D boron

Many reviews have summarized the relevant applications of 2D boron in electronic devices, biomedicine, and energy storage (Han, et al., 2022; Fan et al., 2023; Hou, et al., 2023). However, the catalytic application mechanism has not been systematically discussed. In this section, we focus on 2D boron as harboring active sites and supports for catalysis. We hope that this perspective will shed light on how to develop high-performance catalysts based on 2D boron materials.

3.1 2D boron as catalytic sites

Recently, Kondo *et al*. explored the catalytic activity of HB nanosheets obtained from MgB_2 precursor in the ethanol-reforming reaction (Fujino et al., 2019). The HB catalyst exhibits a distinct ethanol conversion, which increases with the temperature (Fig. 4(a)). By contrast, the precursor MgB_2 and B_2O_3, the main byproduct during the process of HB synthesis, do not show any catalytic performance. In addition, the main product is ethylene (C_2H_4) at various reaction temperatures (Fig. 4(b)), indicating that ethanol reforming by HB nanosheets is a dehydration reaction, as shown in Fig. 4(c). To further explore the reaction mechanism, Kondo *et al*. confirmed the lattice H of HB participating in the dehydration reaction of ethanol by using isotope ethanol with *in situ* Fourier transform infrared (FT-IR) techniques (Fujino et al., 2021). Subsequently, Kondo *et al*. found that the

HB nanosheets as catalysts could also convert CO_2 into CH_4 and C_2H_6 at 423 K under a moist atmosphere (Goto et al., 2022). These results indicate that the HB nanosheets have huge potential as heterogeneous catalysts for energy conversion.

Beyond the above utility 2D boron, it has been proven beneficial for N_2 activation by DFT calculation (Lu et al., 2018). In 2019, Sun and co-authors prepared boron nanosheets (BNS) from a bulk boron precursor by the ultrasonication liquid exfoliation method (Zhang et al., 2019). The prepared BNS was deposited dropwise on carbon paper (BNS/CP) and, for the first time, experimentally employed in the N_2

reduction reaction (NRR). As shown in Fig. 4(d), the BNS/CP exhibited the highest NH_3 yield of 13.22 μg/h/mg$_{cat}$ in 0.1 M Na_2SO_4 among the reported NRR catalysts. Besides, after 2 h of NRR electrolysis, the amount of produced NH_3 for BNS/CP was 2.64 μg, significantly larger than blank CP (0.13 μg) and bulk B/CP (0.17 μg) (Fig. 4(e)). The superior NRR performance of BNS/CP is possible because the catalyst has more active sites and lower charge transfer resistance. Furthermore, the authors confirmed by DFT calculations that the rate-determining step was the desorption process of the second NH_3 molecule (Fig. 4(f)).
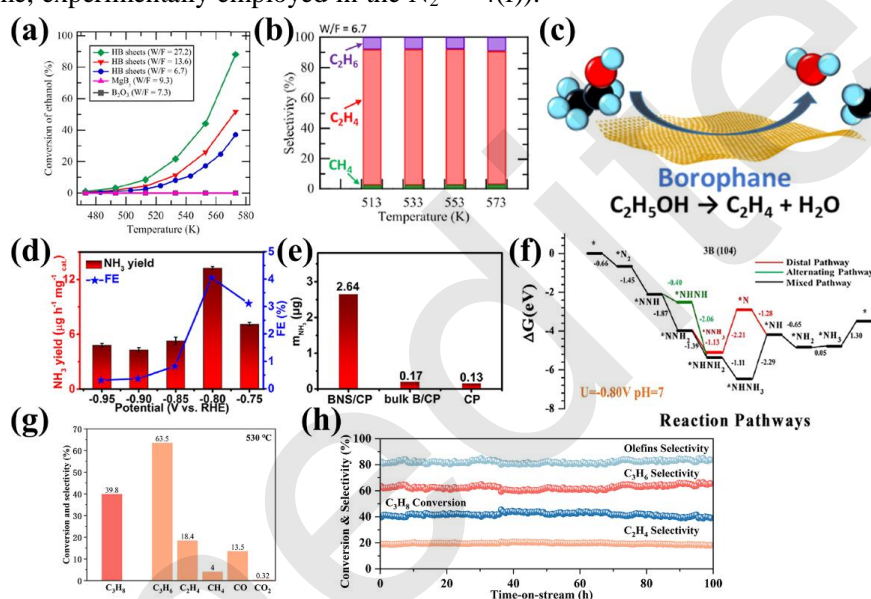

Fig. 4 (a) Ethanol conversion of HB sheets, MgB_2 and B_2O_3 at different temperatures. (b) Selectivity of ethanol reforming by HB as a function of temperature. (c) Schematic illustration of ethanol dehydration on HB sheets. (a-c) Reprinted from (Fujino, et al., 2019) (Copyright 2019, with permission from the American Chemical Society). (d) NH_3 yields and Faraday Efficiencies (FE) for BNS/CP under the corresponding potential. (e) Yields of NH_3 produced with different electrodes at -0.8 V after 2 h of electrolysis. (f) Free-energy diagram of NRR on the B(104) surface. (d-f) Reprinted from (Zhang, et al., 2019) (Copyright 2019, with permission from the American Chemical Society). (g) Catalytic performance of Mg-BNS at 530℃. (h) Stability test of Mg-BNSs at 530℃. (g-h) Reprinted from (Zhang, et al., 2024) (Copyright 2024, with permission from the Royal Society of Chemistry).

Recently, our group prepared boron nanosheets with a few Mg atoms by the chemical exfoliation method, denoted as Mg-BNSs (Zhang, et al., 2024). We explored the catalytic performance of Mg-BNSs in the oxidation dehydrogenation of propane. As shown in Fig. 4(g), the catalysts yielded 39.8% propane conversion, and the propene and ethene selectivities were as high as 63.5% and 18.4%, respectively, at 530℃. Most importantly, the catalysts maintained good stability at 530℃ even after testing

for 100 h (Fig. 4(h)). Based on FT-IR, we identified that the B-H groups on the catalysts converted into B-O groups as the active site during the reaction process.

3.2 2D boron as catalytic supports

Our team has identified abundant Si-H groups on the surface of 2D silicon by chemical exfoliation, which can react with metal ions (Cu^{2+}, Pd^{2+}, Ag^{2+}) to form metal nanoparticles for catalysis (Wang et al., 2020a). Recent research has revealed the similarity of B-H on 2D boron in this reaction. Kondo and

co-workers confirmed that the prepared HB nanosheets had a redox potential between -0.277 and -0.257 V versus standard hydrogen electrode (SHE) by employing ultraviolet-visible spectroscopy. Hence, metal ions with redox potentials larger than -0.257 V can be reduced by HB nanosheets, such as Ni^{2+}, Cu^{2+}, Fe^{3+}, Ag^+, Pd^{2+}, Pt^{2+}, etc. (Ito et al., 2020). For example, the Cu^{2+} from $Cu(CH_3COO)_2$ was reduced by HB nanosheets in acetonitrile solution, and the obtained highly dispersive Cu nanoparticles were approximately 2 nm in size (Fig. 5(a)). Therefore, HB nanosheets may be a useful option for constructing nanocomposite catalysts by acting as both the chemical reductant and the support.

Using HB nanosheets, Yang et al. reduced noble metal ions, such as $PtCl_4^{2-}$, $PdCl_4^{2-}$, and $AuCl_4^-$, to construct electrocatalysts containing noble metal nanoparticles (M/B-C, M = Pt, Pd and Au), as shown in Fig. 5(b) (Gao et al., 2020). It is noteworthy that the amount of noble metal loading reached 52.9 wt%, and the particles were ultrafine-sized (2.9 ± 0.7 nm) and highly dispersed, so that the electrocatalysts exhibited excellent catalytic performance. In addition, they were also highly durable owing to the stronger interaction between noble metal nanoparticles and 2D boron nanosheets. For example, the catalytic performance of Pt/B-C was higher than that of commercial Pt/C catalyst in the oxygen reduction reaction (ORR), methanol oxidation reaction (MOR), and hydrogen evolution reaction (HER) systems. It also maintained the potential of 0.6 V over 72 h in the H_2-O_2 fuel cell (Fig. 5(c)). Yang and co-workers confirmed by DFT calculation that the strength of the Pt-B bond was more than 5 times of Pt-C (Zeng et al., 2023). Based on the robust Pt-B bonds, the authors modulated the metal precursors to synthesize the binary, ternary, quaternary, and quinary Pt intermetallic compound nanocatalysts. Compared with the reported carbon-supported intermetallic PtM nanoparticles, the PtM/B/C catalysts had smaller nanoparticle sizes at around 4 nm (Fig. 5(d)). Such small size enables higher ORR activity than commercial Pt/C (Fig. 5(e)).

Beyond the above strategies, Saad *et al.* employed HB nanosheets as a support for OER catalysts (Saad et al., 2021). The B-H groups on the surface of HB reduced Ag^+ to form Ag nanoparticles with an average size of 7 nm. The as-formed Ag nanoparticles were used as seeds to grow Co_3O_4 nanoplates on the surface of HB support, denoted as Co_3O_4-Ag@B. The authors discovered that the interaction between boron nanosheets and Co_3O_4 could enhance the stability and activity of Co_3O_4-Ag@B in the OER reaction. Compared with the control sample with reduced graphene oxides (rGO) as the support, Co_3O_4-Ag@B showed a lower overpotential of 60 mV and a lower Tafel slope of 27 mV dec^{-1} (Fig. 5(f)). Besides, the overpotentials (η) for Co_3O_4-Ag@B to deliver 30 and 100 mA cm^{-2} current density were small, 307 and 350 mV, respectively, lower than those for Co_3O_4-Ag@rGO (380 and 440 mV). The result of DFT calculation further indicated that the Co_3O_4-Ag@B had a lower energy barrier with 0.12 eV for the intermediate conversion process than the Co_3O_4-Ag@rGO, owing to the formation of Co-B and B-O bonds with the HB nanosheet support (Fig. 5(g)).

Overall, it is a promising approach to synthesize nano-compound catalysts by employing boron nanosheets as support. The strong interaction between boron nanosheets and metal nanoparticles promotes the stability and activity of catalysts, providing huge potential value and wide application prospects in energy conversion and catalysis.
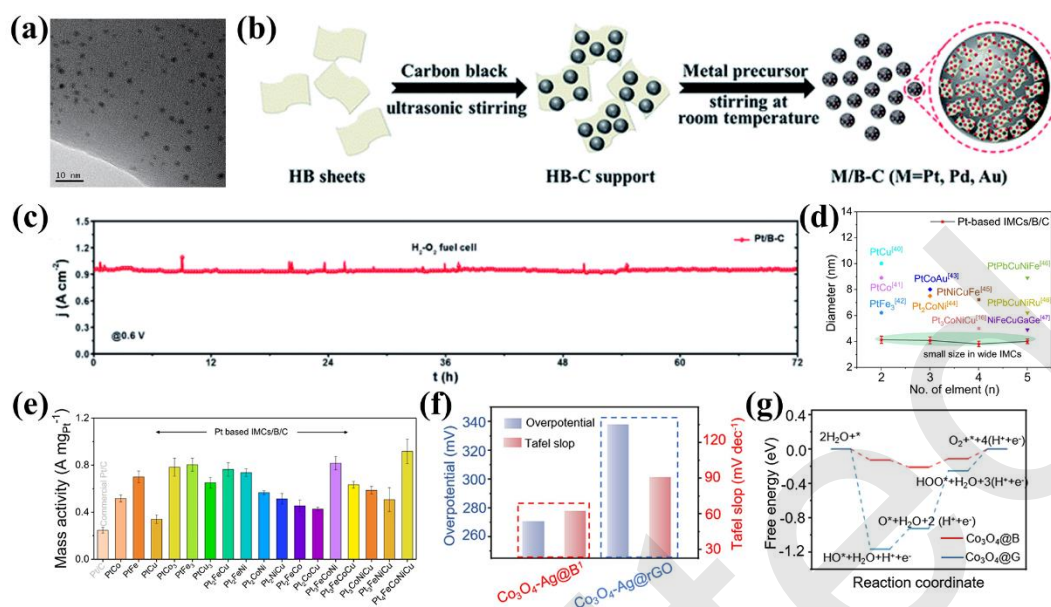
Fig. 5 (a) TEM image of Cu nanoparticles on a HB nanosheet. Reprinted from (Ito, et al., 2020) (Copyright 2020, with permission from The Chemical Society of Japan). (b) Schematic illustration of the synthetic process of M/B-C. (c) H_2-O_2 fuel cell durability test of Pt/B-C at 0.6 V for 72 h. (b-c) Reprinted from (Gao, et al., 2020) (Copyright 2020, with permission from the Royal Society of Chemistry. (d) Comparison of intermetallic alloy size between Pt-based intermetallic compounds with the reported works. (e) The mass activity of commercial Pt/C and Pt-M/B/C for ORR. (d-e) Reprinted from (Zeng, et al., 2023) (Copyright 2023, with permission from Nature Research). (f) The overpotentials and Tafel slopes to achieve 10 mA cm^{-2} for Co_3O_4-Ag@B and Co_3O_4-Ag@rGO catalysts. (g) Reaction free energy diagram for OER on Co_3O_4/B and Co_3O_4/graphene. (f-g) Reprinted from (Saad, et al., 2021) (Copyright 2021, with permission from Elsevier).

4 Summary and Perspective

This mini-review summarizes the synthesis of 2D boron nanosheets by using the top-down method, including chemical exfoliation, cation exchange, and physical exfoliation. The obtained 2D boron nanosheets have been successfully applied in energy conversion and catalysis. Thanks to the added functional groups, 2D boron nanosheets exhibit excellent catalytic performance in ethanol conversion, CO_2 conversion, N_2 reduction reaction, and the oxidation dehydrogenation of propane as active sites. In addition, B-H groups on the surface of 2D boron nanosheets have been demonstrated to be direct reductants for several metal ions. The interaction between the thus formed metal nanoparticles and 2D boron nanosheets can increase the stability of nano-compound catalysts and enhance their activity. Therefore, 2D boron nanosheets can be considered ideal catalytic supports and catalysts (Table 1). Inspired by these pioneering research works on 2D boron nanosheets, we propose some perspectives to broaden this field.

Table 1. Summary of 2D boron heterogeneous catalysts in the recent literatures

Entry	Catalyst	As catalytic support	As catalytic site	Reference
1	HB nanosheets	/	Ethanol conversion	(Fujino, et al., 2019)
2	HB nanosheets	/	CO_2 conversion	(Goto, et al., 2022)
3	BNS/CP	/	N_2 reduction reaction	(Zhang, et al., 2019)
4	Mg-BNSs	/	oxidation dehydrogenation of propane	(Zhang, et al., 2024)
5	Pt/B-C	Oxygen reduction reaction	/	(Gao, et al., 2020)
6	PtM/B/C	Oxygen reduction reaction	/	(Zeng, et al., 2023)
7	Co_3O_4-Ag@B	Oxygen evolution reaction	/	(Saad, et al., 2021)

First, although chemical exfoliation is a facile strategy to synthesize 2D boron nanosheets, it cannot prepare nanosheets with pure boron. For instance, the obtained boron nanosheets have many residual metal atoms when employing acid etching of MgB_2 or AlB_2. To further extract metal ions, it may be a promising route to combine the acid etching method with chelation-assisted and oxidizing strategies. Chelation agents with high affinity for Mg^{2+} or Al^{3+} may facilitate the exsolution of these cations, while oxidizing agents (e.g., metal ions used for exfoliating $CaSi_2$ for the synthesis of 2D Si nanosheets) may help break the ionic Mg-B bonds by annihilating the negative charges of boron. In addition, many metal borides (such as Ni_2B, Cu_2B, Mo_2B, etc.) also have huge potential for preparing 2D boron as the precursors. What is more, some metal borides with layered structures can be directly used for high-performance catalysis (Li et al., 2023).

Second, many functional groups (including hydride, hydroxyl, oxy-functional groups, etc.) can be simultaneously attached to the surface of boron sheets by top-down approaches from bulk boron or MgB_2. These functional groups can not only stabilize the boron nanosheets but also tune their properties. For instance, the OH group can tune the band gap of boron nanosheet due to the hybridization of the oxygen *p* orbital with the boron *p* orbital, which renders the B-OH nanosheets potential value in photo-detection (Wang et al., 2020b). In addition, Sun et al. prepared boron nanosheets from bulk boron in IPA solvent. They found that the oxidized and H-deactivated boron nanosheets could catalyze the NRR more effectively than pristine boron nanosheets (Zhang, et al., 2019). Therefore, it is worth exploring suitable target reactions that can maximize the functions of these groups and identify their specific roles in more versatile energy conversion and catalytic applications.

Finally, the emerging strong metal-support interaction (SMSI) between boron nanosheets and metal nanoparticles is a distinct class from traditional SMSI systems that often involve reducible oxides. This results in exceptionally high loading capacity, stability and dispersion of nanoparticles, conducive to high-performance catalysis. Our recent success in embedding metal nanoparticles into 2D Si nanosheets for highly stable reversed water gas shift reaction also suggests that such SMSI structure has an innate catalytic advantage (Wang, et al., 2022b). However, the mechanism of SMSI formation between boron and metal remains unknown. It is certainly of interest to illustrate the evolutionary process of metal-B bonds (and metal-O, B-O bonds when oxygen is involved in the reaction), which deserves further

exploration through *in-situ* characterization and theoretical simulation.

To conclude, 2D boron is a treasure trove for energy catalysis. Its potential for the advanced catalytic systems has just emerged but has been underpinned by recent demonstrative works. Its sustainable development and further exploitation will be contingent on judicious design of the materials synthetic methods that likely involve the facile and productive top-down approaches. Bearing both the functional groups and metal sites that can participate in the reactions, the obtained boron nanosheets may be excellent options for boosting catalytic performance.

Acknowledgments

Author contributions

W.S. and D.Z. proposed the topic of the review. W.S. and D.Z. wrote and revised the manuscript. C.Z. applied for the copyrights of figures. S. W summarized these figures. All authors contributed to discussion and manuscript review.

Conflict of interest

The authors declare no competing interests.

References:

Cai C, Xiong F, Dong M, et al., 2022. Scalable synthesis of hydroxyl-functionalized boron nanosheets for high ion-conductive solid-state electrolyte applications. *Chem. Commun.*, 58(37):5586-5589.
https://doi.org/10.1039/d2cc00690a

Chahal S, Ranjan P, Motlag M, et al., 2021. Borophene via micromechanical exfoliation. *Adv. Mater.*, 33(34):2102039.
https://doi.org/10.1002/adma.202102039

Chand H, Kumar A, Bhumla P, et al., 2022. Scalable production of ultrathin boron nanosheets from a low-cost precursor. *Adv. Mater. Interfaces*, 9(23):2200508.
https://doi.org/10.1002/admi.202200508

Das SK, Bedar A, Kannan A, et al., 2015. Aqueous dispersions of few-layer-thick chemically modified magnesium diboride nanosheets by ultrasonication assisted exfoliation. *Sci. Rep.*, 5(1):10522.
https://doi.org/10.1038/srep10522

Das SK, Jasuja K, 2018. Chemical exfoliation of layered magnesium diboride to yield functionalized nanosheets and nanoaccordions for potential flame retardant applications. *ACS Appl. Nano Mater.*, 1(4):1612-1622.
https://doi.org/10.1021/acsanm.8b00101

Fan FR, Wang R, Zhang H, et al., 2021. Emerging beyond-graphene elemental 2D materials for energy and catalysis applications. *Chem. Soc. Rev.*, 50(19):10983-11031.
https://doi.org/10.1039/c9cs00821g

Fan M, Liang X, Li Q, et al., 2023. Boron: A key functional component for designing high-performance heterogeneous catalysts. *Chin. Chem. Lett.*, 34(1):107275.
https://doi.org/10.1016/j.cclet.2022.02.080

Fujino A, Ito S-I, Goto T, et al., 2019. Hydrogenated borophene shows catalytic activity as solid acid. *ACS Omega*, 4(9):14100-14104.
https://doi.org/10.1021/acsomega.9b02020

Fujino A, Ito S-I, Goto T, et al., 2021. Ethanol–ethylene conversion mechanism on hydrogen boride sheets probed by in situ infrared absorption spectroscopy. *Phys. Chem. Chem. Phys.*, 23(13):7724-7734.
https://doi.org/10.1039/d0cp03079a

Gao S, Zhang Y, Bi J, et al., 2020. 2D hydrogenated boride as a reductant and stabilizer for in situ synthesis of ultrafine and surfactant-free carbon supported noble metal electrocatalysts with enhanced activity and stability. *J. Mater. Chem. A*, 8(36):18856-18862.
https://doi.org/10.1039/d0ta06542k

Goto T, Ito S-I, Shinde SL, et al., 2022. Carbon dioxide adsorption and conversion to methane and ethane on hydrogen boride sheets. *Commun. Chem.*, 5(1):118.
https://doi.org/10.1038/s42004-022-00739-8

Han C, Han R, Zhang X, et al., 2022. 2D boron nanosheet architectonics: Opening new territories by smart functionalization. *J. Mater. Chem. A*, 10(6):2736-2750.
https://doi.org/10.1039/d1ta09562e

Hou C, Tai G, Wu Z, et al., 2020. Borophene: Current status, challenges and opportunities. *ChemPlusChem*, 85(9):2186-2196.
https://doi.org/10.1002/cplu.202000550

Hou C, Tai G, Liu Y, et al., 2023. Borophene-based materials for energy, sensors and information storage applications. *Nano Research Energy*, 2:e9120051.
https://doi.org/10.26599/nre.2023.9120051

Ito S-I, Hirabayashi T, Ishibiki R, et al., 2020. Hydrogen boride sheets as reductants and the formation of nanocomposites with metal nanoparticles. *Chem. Lett.*, 49(7):789-793.
https://doi.org/10.1246/cl.200206

James AL, Jasuja K, 2017. Chelation assisted exfoliation of layered borides towards synthesizing boron based nanosheets. *RSC Adv.*, 7(4):1905-1914.
https://doi.org/10.1039/c6ra26658d

Ji X, Kong N, Wang J, et al., 2018. A novel top‑down synthesis of ultrathin 2d boron nanosheets for

multimodal imaging-guided cancer therapy. *Adv. Mater.*, 30(36) https://doi.org/10.1002/adma.201803031

Kawamura R, Yamaguchi A, Shimada C, et al., 2020. Acid assisted synthesis of hb sheets through exfoliation of MgB_2 bulk in organic media. *Chem. Lett.*, 49(10):1194-1196. https://doi.org/10.1246/cl.200203

Li H, Jing L, Liu W, et al., 2018. Scalable production of few-layer boron sheets by liquid-phase exfoliation and their superior supercapacitive performance. *ACS Nano*, 12(2):1262-1272. https://doi.org/10.1021/acsnano.7b07444

Li X, Li Z-Q, Liu H-Y, et al., 2023. Theoretical study on hydrogen evolution reaction in transition metal borides. *Rare Metals*, 42(6):1808-1812. https://doi.org/10.1007/s12598-022-02251-3

Liu H, Neal AT, Zhu Z, et al., 2014. Phosphorene: An unexplored 2D semiconductor with a high hole mobility. *ACS Nano*, 8(4):4033-4041. https://doi.org/10.1021/nn501226z

Liu Y, Penev ES, Yakobson BI, 2013. Probing the synthesis of two‐dimensional boron by first‐principles computations. *Angew. Chem. Int. Ed.*, 52(11):3156-3159. https://doi.org/10.1002/anie.201207972

Lu J-B, Ma X-L, Wang J-Q, et al., 2018. Efficient nitrogen fixation via a redox-flexible single-iron site with reverse-dative iron → boron σ bonding. *J. Phys. Chem. A*, 122(18):4530-4537. https://doi.org/10.1021/acs.jpca.8b02089

Ma D, Zhao J, Xie J, et al., 2020. Ultrathin boron nanosheets as an emerging two-dimensional photoluminescence material for bioimaging. *Nanoscale Horiz.*, 5(4):705-713. https://doi.org/10.1039/c9nh00698b

Mannix AJ, Zhou X-F, Kiraly B, et al., 2015. Synthesis of borophenes: Anisotropic, two-dimensional boron polymorphs. *Science*, 350(6267):1513-1516. https://doi.org/10.1126/science.aad1080

Nagamatsu J, Nakagawa N, Muranaka T, et al., 2001. Superconductivity at 39 K in magnesium diboride. *Nature*, 410(6824):63-64. https://doi.org/10.1038/35065039

Nishino H, Fujita T, Cuong NT, et al., 2017a. Formation and characterization of hydrogen boride sheets derived from MgB_2 by cation exchange. *J. Am. Chem. Soc.*, 139(39):13761-13769. https://doi.org/10.1021/jacs.7b06153

Nishino H, Fujita T, Yamamoto A, et al., 2017b. Formation mechanism of boron-based nanosheet through the reaction of MgB_2 with water. *J. Phys. Chem. C*, 121(19):10587-10593. https://doi.org/10.1021/acs.jpcc.7b02348

Novoselov KS, Geim AK, Morozov SV, et al., 2004. Electric field effect in atomically thin carbon films. *Science*, 306(5696):666-669.

https://doi.org/10.1126/science.1102896

Ou M, Wang X, Yu L, et al., 2021. The emergence and evolution of borophene. *Adv. Sci.*, 8(12) https://doi.org/10.1002/advs.202001801

Qian C, Sun W, Hung DLH, et al., 2018. Catalytic CO_2 reduction by palladium-decorated silicon–hydride nanosheets. *Nat. Catal.*, 2(1):46-54. https://doi.org/10.1038/s41929-018-0199-x

Radisavljevic B, Radenovic A, Brivio J, et al., 2011. Single-layer mos_2 transistors. *Nat. Nanotechnol.*, 6(3):147-150. https://doi.org/10.1038/nnano.2010.279

Saad A, Liu D, Wu Y, et al., 2021. Ag nanoparticles modified crumpled borophene supported Co_3O_4 catalyst showing superior oxygen evolution reaction (OER) performance. *Appl. Catal., B*, 298:120529. https://doi.org/10.1016/j.apcatb.2021.120529

Su Y, Wang S, Ji L, et al., 2023. High surface area siloxene for photothermal and electrochemical catalysis. *Nanoscale*, 15(1):154-161. https://doi.org/10.1039/d2nr05140k

Sun R, Chen J, Zhang W, et al., 2023. Facile synthesis of oxidized boron nanosheets for chemo- and biosensing. *Anal. Chem.*, 95(30):11475-11482. https://doi.org/10.1021/acs.analchem.3c01979

Tominaka S, Ishibiki R, Fujino A, et al., 2020. Geometrical frustration of B-H bonds in layered hydrogen borides accessible by soft chemistry. *Chem*, 6(2):406-418. https://doi.org/10.1016/j.chempr.2019.11.006

Wang C, Xu X, Pi X, et al., 2022a. Neuromorphic device based on silicon nanosheets. *Nat. Commun.*, 13(1) https://doi.org/10.1038/s41467-022-32884-y

Wang S, Wang C, Pan W, et al., 2020a. Two‐dimensional silicon for (photo)catalysis. *Solar RRL*, 5(2):2000392. https://doi.org/10.1002/solr.202000392

Wang S, Feng K, Zhang D, et al., 2022b. Stable cu catalysts supported by two-dimensional SiO_2 with strong metal–support interaction. *Adv. Sci.*, 9(9):2104972. https://doi.org/10.1002/advs.202104972

Wang X, Liang J, You Q, et al., 2020b. Bandgap engineering of hydroxy-functionalized borophene for superior photo-electrochemical performance. *Angew. Chem. Int. Ed.*, 59(52):23559-23563. https://doi.org/10.1002/anie.202010723

Xie Z, Duo Y, Fan T, et al., 2022. Light-induced tumor theranostics based on chemical-exfoliated borophene. *Light: Sci. Appl.*, 11(1):324. https://doi.org/10.1038/s41377-022-00980-9

Zeng X, Jing Y, Gao S, et al., 2023. Hydrogenated borophene enabled synthesis of multielement intermetallic catalysts. *Nat. Commun.*, 14(1):7414. https://doi.org/10.1038/s41467-023-43294-z

Zhang D, Wang S, Zhang C, et al., 2024. Chemically exfoliated boron nanosheets for efficient oxidative

dehydrogenation of propane. *Nanoscale*, https://doi.org/10.1039/d3nr05212e

Zhang F, Jia C, Zhang N, et al., 2022. Few-layer mg-deficient borophene nanosheets: I_2 oxidation and ultrasonic delamination from MgB_2. *Nanoscale*, 14(11):4195-4203. https://doi.org/10.1039/d1nr07353b

Zhang X, Wu T, Wang H, et al., 2019. Boron nanosheet: An elemental two-dimensional (2D) material for ambient electrocatalytic N_2-to-NH_3 fixation in neutral media. *ACS Catal.*, 9(5):4609-4615. https://doi.org/10.1021/acscatal.8b05134

Zhao W, Ghorannevis Z, Chu L, et al., 2012. Evolution of electronic structure in atomically thin sheets of WS_2 and WSe_2. *ACS Nano*, 7(1):791-797. https://doi.org/10.1021/nn305275h